

# Beryllium abundances in metal-poor stars <sup>★</sup>

K. F. Tan<sup>1,2†</sup>, J. R. Shi<sup>1</sup> and G. Zhao<sup>1</sup>

<sup>1</sup>*National Astronomical Observatories, Chinese Academy of Sciences, Beijing 100012, China*

<sup>2</sup>*Graduate University of the Chinese Academy of Sciences, Beijing 100049, China*

Accepted ?. Received ?; in original form ?

## ABSTRACT

We have determined beryllium abundances for 25 metal-poor stars based on the high resolution and high signal-to-noise ratio spectra from the VLT/UVES database. Our results confirm that Be abundances increase with Fe, supporting the global enrichment of Be in the Galaxy. Oxygen abundances based on [O I] forbidden line implies a linear relation with a slope close to one for the Be vs. O trend, which indicates that Be is probably produced in a primary process. Some strong evidences are found for the intrinsic dispersion of Be abundances at a given metallicity. The deviation of HD 132475 and HD 126681 from the general Be vs. Fe and Be vs. O trend favours the predictions of the superbubble model, though the possibility that such dispersion originates from the inhomogeneous enrichment in Fe and O of the protogalactic gas cannot be excluded.

**Key words:** stars: abundances – stars: atmospheres – stars: Population II – Galaxy: evolution – Galaxy: halo

## 1 INTRODUCTION

The light element beryllium (Be) has very special origins. The primordial Be abundance (on the order of  $N(\text{Be}/\text{H}) = 10^{-17}$ , Thomas et al. 1994) is negligible as predicted by the standard Big Bang Nucleosynthesis. Be can not be produced by nuclear fusion in the interiors of stars; on the opposite, Be will be destroyed by this process. It was first proposed by Reeves, Fowler & Hoyle (1970) that Be can be created by spallation reactions between galactic cosmic rays (GCRs) and the CNO nuclei in the interstellar medium (ISM). This model predicts a quadratic relation between the abundances of Be and O (or a slope of 2 in logarithmic plane), assuming that the CNO abundance is proportional to the cumulative number of Type II supernovae (SNeII) and the cosmic ray flux is proportional to the instantaneous rate of SNeII. However, recent observational results (e.g., Gilmore et al. 1992; Boesgaard & King 1993; Molaro et al. 1997) showed a linear relation between Be and O abundances, which indicates that Be may be produced in a primary process instead of the standard secondary GCRs process. Duncan et al. (1997) suggested that Be can be produced in a reverse spallation of C and O nuclei onto protons and  $\alpha$ -particles. This process will lead to a linear dependence of Be on O abundances. The results from the latest big survey by Boesgaard et al.

(1999, hereafter B99) showed that the slope of the Be vs. O trend in logarithmic scale is about 1.5, which makes the Be production scenario more complicated and confusing. In addition, the exact slope of the Be vs. O relationship depends on which oxygen indicator is used (see discussion in Sect. 4.1).

If Be is produced in a primary process and the cosmic rays were transported globally across the early Galaxy, Be abundances should show a very small scatter at a given time. This makes the Be abundance an ideal cosmic chronometer (Suzuki & Yoshii 2001). Pasquini et al. (2004, 2007) found that Be abundances in globular clusters NGC 6397 and NGC 6752 are very similar to that of the field stars with the same Fe abundances. Furthermore, the derived ages from Be abundances based on the model of Valle et al. (2002) are in excellent agreement with the ages determined by main-sequence fitting. They suggested that Be is produced in primary spallation of cosmic rays acting on a Galactic scale, and therefore can be used as a cosmochronometer. However, B99 and Boesgaard & Novicki (2006) found strong evidences for intrinsic spread of Be abundances at a given metallicity, which may indicate that there is also local enrichment of Be in the Galaxy. But interestingly, Pasquini et al. (2005) found that stars belonging to the accretion and dissipative populations (see Gratton et al. 2003 for the exact definitions for these two kinematical classes) are neatly separated in the [O/Fe] vs.  $\log(\text{Be}/\text{H})$  diagram, and especially, the accretion component shows a large scatter in the [O/Fe] vs.  $\log(\text{Be}/\text{H})$  diagram. They proposed that most of the scatter in the Be vs. Fe (O) trend may be attributed to the intrinsic

<sup>★</sup> Based on observations made with the European Southern Observatory telescopes obtained from the ESO/ST-ECF Science Archive Facility.

<sup>†</sup> E-mail: tan@bao.ac.cn

spread of Fe and O abundances (probably due to the inhomogeneous enrichment in Fe and O of the protogalactic gas), rather than Be.

In this work, we present Be abundances of 25 metal-poor stars, for most of which the Be abundances are derived for the first time. Oxygen abundances are also determined from both [O I] forbidden line and O I triplet lines to investigate the chemical evolution of Be with O in the Galaxy. In Sect. 2 we briefly describe the observations and data reduction. The adopted model atmosphere and stellar parameters are discussed in Sect. 3. Sect. 4 deals with the abundances determinations and uncertainties. Sect. 5 presents the results and discussions, and the conclusions are given in the last section.

## 2 OBSERVATIONS AND DATA REDUCTION

Our analysis are based on the high resolution and high signal-to-noise ratio spectra of 25 metal-poor main sequence and subgiant stars from the archive database of observations obtained with UVES, the Ultraviolet and Visual Echelle Spectrograph (Dekker et al. 2000) at the ESO VLT 8 m Kueyen telescope. The spectra were obtained during two observation runs: April 8–12, 2000 and April 10–12, 2001 (Programme ID 65.L-0507 and 67.D-0439), both with standard Dichroic #1 setting in the blue and red arms. The blue arm spectra ranged from 3050 to 3850 Å with a resolution of 48 000, while the red arm spectra ranged from 4800 to 6800 Å with a resolution of 55 000.

The spectra were reduced using the standard ESO MIDAS package. Reduction procedure includes location of echelle orders, wavelength calibration, background subtraction, flat-field correction, order extraction, and continuum normalization.

## 3 MODEL ATMOSPHERES AND STELLAR PARAMETERS

We adopted the one dimensional line-blanketed local thermodynamic equilibrium (LTE) atmospheric model MAFAGS (Fuhrmann et al. 1997) in our analysis. This model utilizes the Kurucz (1992) ODFs but rescales the iron abundance by  $-0.16$  dex to match the improved solar iron abundance of  $\log \varepsilon(\text{Fe}) = 7.51$  (Anders & Grevesse 1989). Individual models for each star were computed with  $\alpha$ -enhancement of 0.4 dex if  $[\text{Fe}/\text{H}] < -0.6$  and with the mixing length parameter  $l/H_p = 0.5$  to get consistent temperatures from the Balmer lines.

The effective temperatures were derived by fitting the wings of H $\alpha$  and H $\beta$  lines, and then averaged. Nissen et al. (2002) studied oxygen abundances of a large sample stars, which includes all the objects investigated in this work (actually our sample is a subset of those employed by Nissen et al. 2002). They determined the effective temperatures from the  $b - y$  and  $V - K$  colour indices based on the infrared flux method (IRFM) calibrations of Alonso, Arribas & Martinez-Roger (1996). As shown by Fig. 1a, the agreement between the two sets of temperatures are good for most of the stars with a mean difference of  $15 \pm 89$  K. For the star G 020-024, Nissen et al. (2002)

**Table 1.** Stellar parameters adopted in the analysis.

Star	$T_{\text{eff}}$ K	$\log g$ cgs	[Fe/H] dex	$\xi$ km s $^{-1}$	Mass $\mathcal{M}_{\odot}$
HD 76932	5890	4.12	-0.89	1.2	0.91
HD 97320	6030	4.22	-1.20	1.3	0.81
HD 97916	6350	4.11	-0.88	1.5	1.03
HD 103723	6005	4.23	-0.82	1.3	0.87
HD 106038	5990	4.43	-1.30	1.2	0.81
HD 111980	5850	3.94	-1.11	1.2	0.83
HD 113679	5740	3.94	-0.70	1.2	0.94
HD 121004	5720	4.40	-0.73	1.1	0.80
HD 122196	5975	3.85	-1.74	1.5	0.81
HD 126681	5595	4.53	-1.17	0.7	0.71
HD 132475	5705	3.79	-1.50	1.4	0.88
HD 140283	5725	3.68	-2.41	1.5	0.79
HD 160617	5940	3.80	-1.78	1.5	0.86
HD 166913	6050	4.13	-1.55	1.3	0.77
HD 175179	5780	4.18	-0.74	1.0	0.85
HD 188510	5480	4.42	-1.67	0.8	0.55
HD 189558	5670	3.83	-1.15	1.2	0.95
HD 195633	6000	3.86	-0.64	1.4	1.11
HD 205650	5815	4.52	-1.13	1.0	0.77
HD 298986	6085	4.26	-1.33	1.3	0.81
CD -30° 18140	6195	4.15	-1.87	1.5	0.79
CD -57° 1633	5915	4.23	-0.91	1.2	0.84
G 013-009	6270	3.91	-2.28	1.5	0.80
G 020-024	6190	3.90	-1.92	1.5	0.83
G 183-011	6190	4.09	-2.08	1.5	0.77

gave a temperature of 6440 K, which is 250 K higher than ours. Recently, Asplund et al. (2006) derived a temperature of 6247 K for G 020-024 based on H $\alpha$  profile fitting, which is very close to ours. Nissen et al. (2002) likely overestimated the reddening of this star (Asplund et al. 2006).

The surface gravities were determined from the fundamental relation

$$\log \frac{g}{g_{\odot}} = \log \frac{\mathcal{M}}{\mathcal{M}_{\odot}} + 4 \log \frac{T_{\text{eff}}}{T_{\text{eff},\odot}} + 0.4(M_{\text{bol}} - M_{\text{bol},\odot}) \quad (1)$$

and

$$M_{\text{bol}} = V + BC + 5 \log \pi + 5 \quad (2)$$

where  $\mathcal{M}$  is the stellar mass,  $M_{\text{bol}}$  is the absolute bolometric magnitude,  $V$  is the visual magnitude,  $BC$  is the bolometric correction, and  $\pi$  is the parallax.

The absolute visual magnitude were directly derived from the *Hipparcos* parallax (ESA 1997) if available with a relative error smaller than 30 per cent. For two stars G 020-024 and G 183-011, their uncertainties in parallaxes are larger than 40 per cent, so only photometric absolute visual magnitude can be adopted. For G 183-011 we followed the  $M_{V,\text{phot}} = 4.08$  from Nissen et al. (2002). While for G 020-024 a large difference exists between the result of Nissen et al. (2002) ( $M_{V,\text{phot}} = 4.33$ ) and that of Asplund et al. (2006) ( $M_{V,\text{phot}} = 3.72$ ). We adopted the latter value because Asplund et al. (2006) used the spectroscopic H $\alpha$  index which provides more precise estimate of interstellar reddening excess than the photometric H $\beta$  index employed by Nissen et al. (2002). The bolometric correction was taken from Alonso, Arribas & Martinez-Roger (1995) and the stellar mass was estimated by comparing its position in the  $\log(L/L_{\odot})$ - $\log T_{\text{eff}}$  diagram with the evolutionary

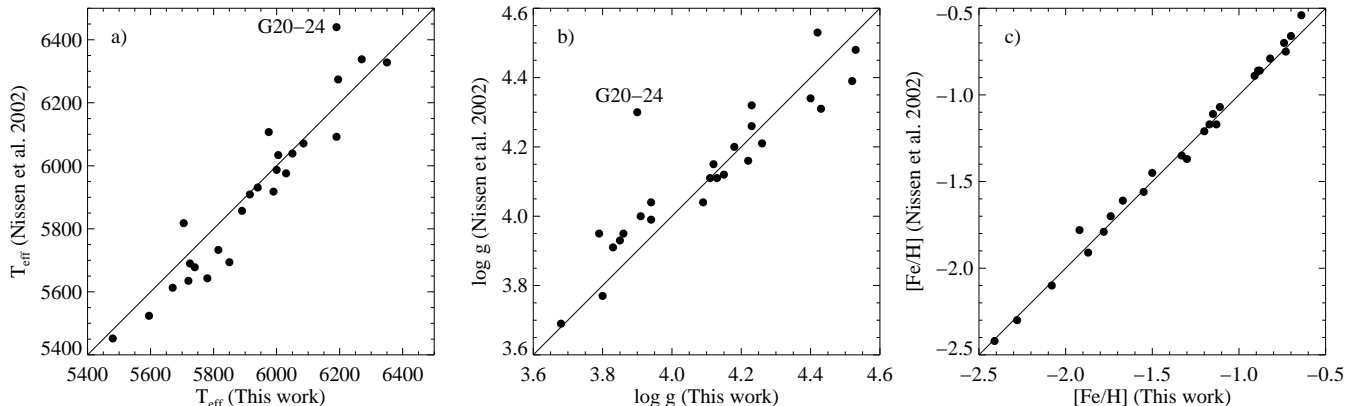


**Figure 1.** Comparison of effective temperature, surface gravity and iron abundance with Nissen et al. (2002).

**Table 2.** Fe II lines used to determine the iron abundances.

Wavelength Å	$E_{\text{low}}$ eV	$\log gf$	$\log C_6$
4993.350	2.79	-3.73	-32.18
5100.664	2.79	-4.18	-31.78
5197.575	3.22	-2.27	-31.89
5234.631	3.21	-2.21	-31.89
5325.560	3.21	-3.21	-32.19
5425.257	3.19	-3.27	-32.19
6084.110	3.19	-3.84	-32.19
6149.250	3.87	-2.76	-32.18
6247.560	3.87	-2.33	-32.18
6416.928	3.87	-2.67	-32.18
6432.680	2.88	-3.61	-32.11
6456.383	3.89	-2.09	-32.18

tracks of Yi, Kim & Demarque (2003). The final  $\log g$  values are given in Table 1. Our results are  $0.03 \pm 0.11$  dex lower than those of Nissen et al. (2002) on average. Good agreement holds on for majority of the stars except for G 020-024, whereas a difference of 0.43 dex exists. This is mainly due to the very different absolute visual magnitude adopted by Nissen et al. (2002) and us as discussed above. The difference in  $M_V$  (0.61 mag) alone will introduce a difference of 0.24 dex to the surface gravity according to Equation (1).

Iron abundances were determined from 12 unblended Fe II lines with spectra synthesis method. We adopted the differential  $\log gf$  values with respect to  $\log \varepsilon(\text{Fe})_{\odot} = 7.51$  from Korn, Shi & Gehren (2003) and the van der Waals damping constants from Anstee & O’Mara (1991, 1995). Our final iron abundances are in excellent agreement with those of Nissen et al. (2002), who also derived the iron abundances from Fe II lines. The mean difference is only  $-0.02 \pm 0.05$  dex. The microturbulent velocities were determined by requiring that the derived  $[\text{Fe}/\text{H}]$  are independent of equivalent widths.

The typical error for our effective temperature is about  $\pm 80$  K. The uncertainty of parallax contributes most to the error of the surface gravity. The typical relative error of  $\pm 15$  per cent in parallax corresponds to an error of  $\pm 0.13$  dex. In addition, the estimated error of  $\pm 0.05 M_{\odot}$  in stellar mass translates to an error of  $\pm 0.02$  dex, while errors of  $\pm 80$  K in effective temperature and  $\pm 0.05$  mag in  $BC$  each

leads to an uncertainty of  $\pm 0.02$  dex. So the total error of  $\log g$  is about  $\pm 0.15$  dex. It is already noted that the iron abundance is insensitive to the effective temperature. The uncertainty of  $[\text{Fe}/\text{H}]$  is dominated by the error of surface gravity. A typical error of  $\pm 0.15$  dex in  $\log g$  results in an error of about  $\pm 0.07$  dex in  $[\text{Fe}/\text{H}]$ . Combined with the line-to-line scatter of about  $\pm 0.03$  dex, the total error of  $[\text{Fe}/\text{H}]$  is about  $\pm 0.08$  dex. And the error for the microturbulent velocity is estimated to be about  $\pm 0.2 \text{ km s}^{-1}$ .

## 4 ABUNDANCES AND UNCERTAINTIES

### 4.1 Oxygen

As Be is mainly produced by the spallation of CNO nuclei, oxygen abundances can be a preferred alternative to iron in investigating the galactic evolution of Be. It is also important to know the O content when determining Be abundances, because there are many OH lines around the Be II doublet. Therefore, the oxygen abundances were firstly investigated here.

There are several indicators for oxygen abundance: the ultraviolet OH, the [O I] 6300 and 6363 Å, the infrared O I 7774 Å triplet and the infrared vibration-rotation OH lines. However, OH molecules and O I atoms in the lower state of the 7774 Å transitions are minority species compared to total number of oxygen atoms, thus are very sensitive to the adopted stellar parameters, such as the effective temperature and surface gravity. Moreover, line formations are far from LTE for either the ultraviolet OH (Hinkle & Lambert 1975; Asplund & García Pérez 2001) or the O I 7774 Å triplet lines (Kiselman 2001). In contrast, [O I] lines are formed very close to LTE and nearly all the oxygen atoms in the photosphere of dwarf and giant stars are in the ground configuration which provide the lower and upper level of the forbidden lines (Nissen et al. 2002). Therefore, it is believed that the [O I] line is the most reliable indicator for oxygen abundances, but the difficulty is that the [O I] lines are very weak in dwarf and subgiant stars.

High resolution and high signal-to-noise ratio spectra covering the infrared O I triplet for 10 stars were available from the archived VLT/UVES spectra database. We re-reduced the spectra and measured the equivalent widths. Since for six of these ten stars O abundances from the O I

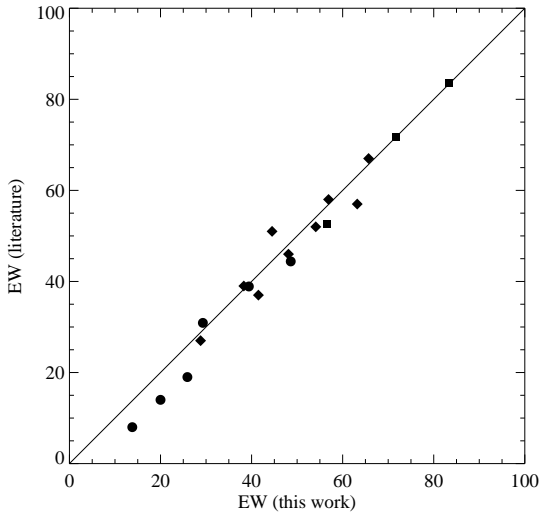


**Figure 2.** Comparison of O I triplet equivalent widths between this work and the literatures (*circles*: Jonsell et al. 2005; *diamonds*: Nissen & Schuster 1997; *squares*: Boesgaard & King 1993).

triplet were previously derived by other authors, we compare our measurements with those found in literature in Fig. 2. It can be seen that the agreement is good on the whole. For the rest 15 stars, we collected their O I 7774 Å triplet equivalent widths from the literatures directly. Oxygen abundances were computed with the  $\log gf = 0.369$ , 0.223, and 0.002 from Wiese, Fuhr & Deters (1996) in LTE first. Then non-LTE corrections were applied according to the results of Takeda (2003).

In addition, Nissen et al. (2002) measured the equivalent widths of [O I] 6300 Å line for 18 main-sequence and subgiant stars, of which 15 stars are included in our sample. They performed the measurement in a very careful fashion, including removing the possible blending telluric O<sub>2</sub> and H<sub>2</sub>O lines with the observed spectra of rapidly rotating B-type stars and subtracting the equivalent width of the blending Ni I line at 6300.339 Å. The typical error for the equivalent width of [O I] 6300 Å line was estimated to be about only  $\pm 0.3$  mÅ. For these 15 stars, we also determined their oxygen abundances with the equivalent widths of [O I] 6300 Å line from Nissen et al. (2002) using the accurate oscillator strength  $\log gf = -9.72$  from Allende Prieto, Lambert & Asplund (2001).

Finally, we derived the oxygen abundances with O I 7774 Å triplet for all the 25 sample stars and with [O I] 6300 Å line for 15 stars, which are given in Table 3 (the reference solar O abundance is  $\log \varepsilon(\text{O}) = 8.77$  computed from [O I] 6300 Å line using the equivalent width of 4.1 mÅ from Nissen et al. 2002).

Oxygen abundance from the weak [O I] 6300 Å line is not sensitive to stellar parameters. Its uncertainty is dominated by the error in equivalent width. Normally, a typical error of  $\pm 0.3$  mÅ in equivalent width corresponds on average to an error of  $\pm 0.1$  dex in oxygen abundance. For the infrared O I triplet, errors of  $\pm 80$  K in effective temperature and  $\pm 0.15$  dex in gravity each translates to an error of  $\pm 0.05$  dex in oxygen abundance. The uncertainties in iron abundance and microturbulence nearly have no effect on

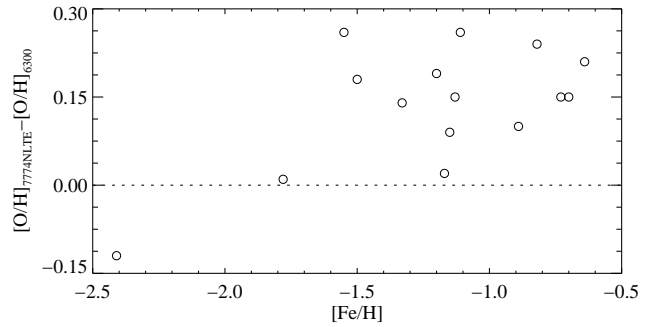


**Figure 3.** Comparison of O abundances from [O I] 6300 Å line with those from O I 7774 Å lines.

[O/Fe]. A typical error of  $\pm 3$  mÅ in equivalent width corresponds to an error of  $\pm 0.04$  dex. In total, the error of [O/Fe] from O I triplet is around  $\pm 0.08$  dex. The uncertainty stated above is a random one, and the systematic error can be much higher, as can be seen from the differences of O abundances between [O I] forbidden line and O I triplet lines discussed below.

As there are 15 stars with oxygen abundances from both [O I] 6300 Å and O I 7774 Å lines, it is interesting to investigate whether these two indicators give consistent oxygen abundances. Fig. 3 shows the differences of O abundances based on [O I] 6300 Å and O I 7774 Å lines. We find that, on average, O abundances from O I 7774 Å lines with NLTE corrections are  $0.14 \pm 0.10$  dex higher than those from [O I] 6300 Å line for the 15 sample stars, which means that these two indicators are not consistent in our study. Nissen et al. (2002) found that the mean difference between O abundance from the forbidden and permitted lines is only 0.03 dex for five of their stars, and they concluded that these two indicators produce consistent O abundances. As a test, we reanalyse the O abundances of Nissen et al. (2002)'s sample using their stellar parameters and equivalent widths. The only differences are the adopted model atmospheres and the NLTE corrections for the O I triplet lines. We found that, for the forbidden line, our abundances are almost the same as those from Nissen et al. (2002), but for the triplet lines, our mean LTE O abundance is about 0.06 dex larger than that of Nissen et al. (2002), and the NLTE correction for the triplet lines from Takeda (2003) is 0.06 dex lower than theirs. These two factors lead to a total difference of 0.12 dex for the permitted lines. Therefore, the different model atmospheres (MAFAGS vs. MARCS) and NLTE corrections are responsible for the differences. Recently, García Pérez et al. (2006) determined O abundances for 13 subgiant stars with [O I], O I and OH lines. They followed exactly the same method as Nissen et al. (2002), but their results showed that O abundances based on O I triplet are on average  $0.19 \pm 0.22$  dex higher than that from the forbidden line.

## 4.2 Beryllium

Beryllium abundances were derived by spectra synthesis of the Be II 3130 Å resonance doublet region using the IDL/FORTRAN SIU software package of Reetz (1993). It is well known that this spectral region is rich with atomic and molecular lines for solar-type stars, which results in substantial line absorption and a deficit of con-

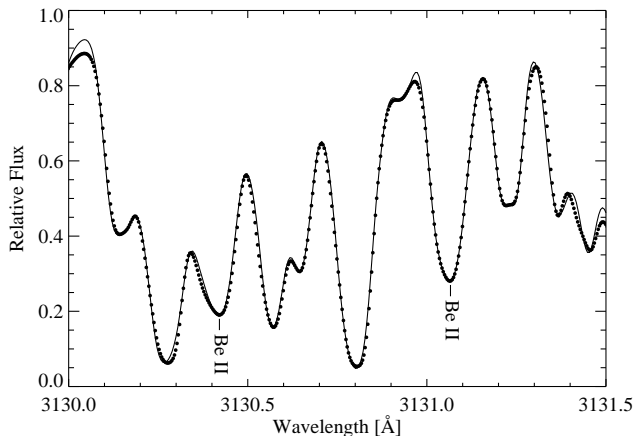


**Figure 4.** Spectral synthesis of the Be II doublet region for the KPNO Solar Flux Atlas data.

tinuum. We firstly computed the synthetic solar spectrum around Be II doublet region based on the line list carefully compiled and tested by Primas et al. (1997), and then compared them with the integrated solar flux atlas of Kurucz et al. (1984). Some changes were made in order to make the theoretical solar spectrum match the Kurucz et al. (1984) solar flux atlas best. The major change made to the Primas et al. (1997) line list is that we increased the  $\log gf$  of the Mn II 3131.017 Å line by 1.72 dex instead of adding a predicted Fe I line at 3131.043 Å. Similar adjustment was adopted by King, Deliyannis & Boesgaard (1997). Based on this adjusted line list, we reproduced the solar flux atlas best with  $A(\text{Be}) = 1.12$ , which is in good agreement with the result of  $A(\text{Be}) = 1.15 \pm 0.20$  derived by Chmielewski, Braut & Mueller (1975). Balachandran & Bell (1998) found that the standard UV continuous opacity of the sun need to be multiplied by a factor of 1.6 in order to get consistent oxygen abundances from the UV and IR OH lines. With the increased UV continuous opacity, they determined the solar Be abundance to be 1.40, which is very close to the meteoritic value 1.42. Bell, Balachandran & Bautista (2001) proposed later that the ‘missing’ UV opacity could be accounted for by the Fe I bound-free transitions. However, until now there is no confirmed evidence about this. But one should keep in mind the ‘missing’ UV opacity problem. If it does exist, the Be vs. Fe (O) trend of this work and all the previous work based on the standard UV opacity might change.

In addition to some strong OH lines, a strong Ti II line at 3130.810 Å also presents in the Be II region. In order to minimize its effect on the beryllium abundance as well as to provide a constraint on the location of continuum, we derived the Ti abundances for our sample stars from the Ti I 5866.461, 6258.110, and 6261.106 Å lines. The oscillator strengths for these lines are differentially adjusted to produce the solar Ti abundance  $\log \varepsilon(\text{Ti}) = 4.94$ . For five very metal-poor stars with  $[\text{Fe}/\text{H}] < -1.8$ , the Ti I lines are too weak to be detected, thus a common value of  $[\text{Ti}/\text{Fe}] = 0.35$  (Magain 1989) was adopted. As a matter of fact, due to the metal deficiency of these stars, the line blending and continuum normalization were much less problematic than solar-type stars. The abundances of other elements, which are less critical for Be abundance deter-

mination, were adopted by scaling a solar composition. Beryllium abundances were then determined by varying the value of Be to best fit the observed line profiles. It was reported by García López, Severino & Gomez (1995) and Kiselman & Carlsson (1996) that non-LTE effects for Be II doublet are insignificant, normally smaller than 0.1 dex. We took the weaker 3131.066 Å line as the primary abundance indicator because it’s less blended compared to the stronger 3130.421 Å component.

The uncertainties of Be abundances were estimated from the errors of stellar parameters and pseudo-continuum location. An error of  $\pm 0.15$  dex in surface gravity implies uncertainties of  $\pm(0.06-0.09)$  dex, while an uncertainty of  $\pm 0.08$  dex in  $[\text{Fe}/\text{H}]$  corresponds to an error of  $\pm 0.06$  dex. Errors due to effective temperature and microturbulence are always within  $\pm 0.04$  dex in total. The error in continuum location was estimated to be less than five per cent in the worst case, which results in an error of  $\pm 0.15$  dex at most. The final errors for each star are given in Table 3.

Be abundances for several stars of our sample have been published by other authors and they are summarized in Table 4. We can see that, though relatively large scatter exists, Be abundances from different researches are not different within uncertainties for majority of the stars. The exceptions are HD 160617 and HD 189558. Our Be abundance of HD 160617 is 0.5 dex higher than that of Molaro et al. (1997). This difference is mostly due to the different stellar parameters adopted by Molaro et al. (1997) and us. Their effective temperature and surface gravity are 276 K and 0.51 dex lower than ours, respectively, which result in a much lower Be abundance. Another exception is HD 189558, where a difference of 0.37 dex in Be abundance exists between the result of Boesgaard & King (1993) and ours. The slight differences in the adopted stellar parameters could not produce such a large difference. Rebolo et al. (1988) derived a Be abundance of  $\log N(\text{Be}/\text{H}) = -12.0 \pm 0.4$  dex for this star with similar stellar parameters. It is 1 dex lower than the result of Boesgaard & King (1993). We noted that Boesgaard & King (1993) determined Be abundances by measuring the equivalent width of Be II doublet, which is very sensitive to the location of the continuum. It is probably that they overestimated the continuum. Moreover, both the spectra of Molaro et al. (1997) and Boesgaard & King (1993) were obtained with 3.6 m telescopes. The signal-to-noise ratios around Be II region of their spectra are much lower than that of this work.

### 4.3 Lithium

It is well known that beryllium can be destroyed in stars by fusion reactions at a relatively low temperature (about 3.5 million K). In order to avoid contamination of our sample from the effect of depletion process in stars, we also determined the  ${}^7\text{Li}$  abundances for our sample stars. Because the destruction temperature for  ${}^7\text{Li}$  is lower than that of Be, if  ${}^7\text{Li}$  is not depleted, Be should not be depleted either<sup>1</sup>.

<sup>1</sup> For subgiant stars, Li and Be can be diluted due to the enlargement of the convection zone. In this case, Li and Be will be diluted by the same percentage. Nevertheless, Be cannot be depleted more than Li in any case.

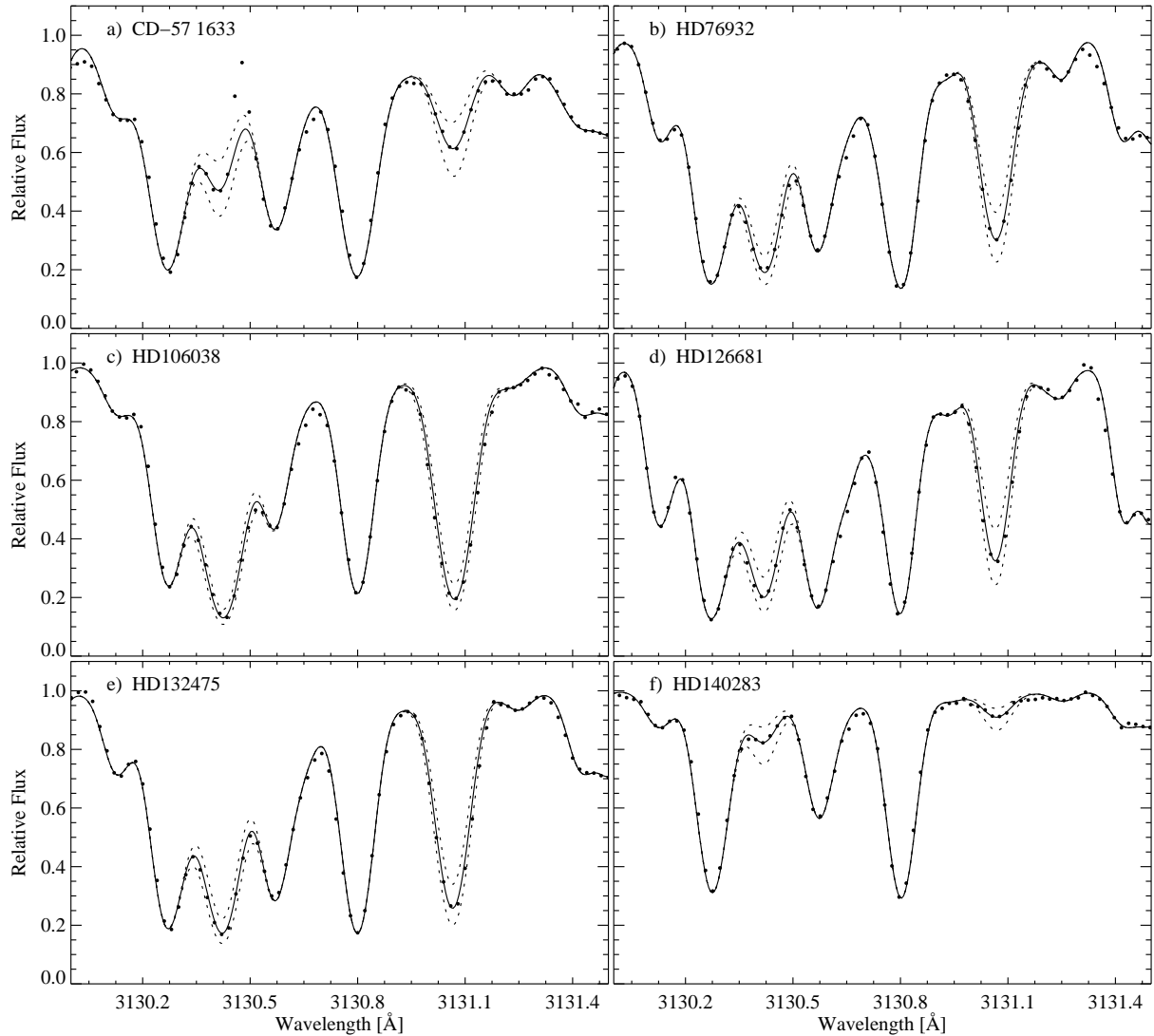


**Figure 5.** Spectrum synthesis for six representative stars. The dots are the observational data, the solid line is the best-fit synthesis, and the dotted lines are synthetic spectra with Be abundances of  $\pm 0.2$  dex relative to the best fit.

We adopted the oscillator strengths from the NIST data base, namely  $\log gf = 0.002$  and  $-0.299$  for the Li I 6707.76 and 6707.91 Å lines, respectively. Collisional broadening parameters describing van der Waals interaction with hydrogen atoms were taken from Barklem, O’Mara & Ross (1998) (see Shi et al. 2007 in detail). Li abundances were derived by spectra synthesis in LTE. Results from Asplund et al. (2006) and Shi et al. (2007) showed that non-LTE effects for Li I resonance lines are insignificant. The typical error for our Li abundance was estimated to be about 0.1 dex.

## 5 RESULTS AND DISCUSSION

### 5.1 Be vs. Fe and Be vs. O relation

Encouraged by the agreement of Be abundances between our results and literatures, we now turn to investigate the chemical evolution of beryllium in the Galaxy. As we have mentioned before, it is first necessary to investigate whether some of our stars are depleted in Be. Fig. 6 displays the

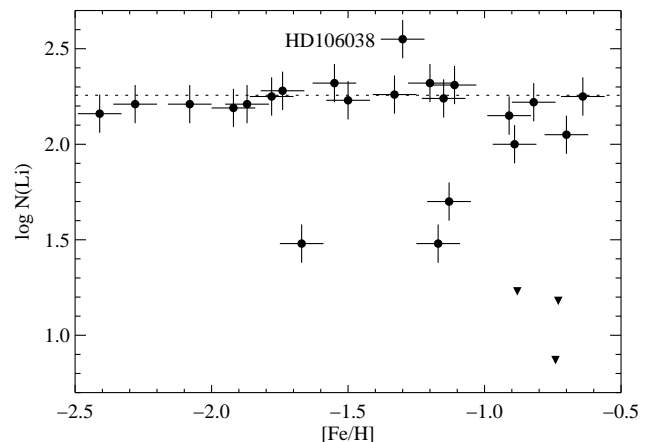


**Figure 6.** Li abundances as a function of  $[\text{Fe}/\text{H}]$ . The filled circles are the determined Li abundances, while the inverse triangles represent the upper limit.

**Table 3.** Abundances and population membership.

Star	[Fe/H]	[O/H]			[Ti/Fe]	A(Li)	A(Be)	$\sigma$ (Be)	Pop. <sup>b</sup>
		6300	7774 LTE <sup>a</sup>	7774 <i>n</i> -LTE					
HD 76932	-0.89	-0.46	-0.24 <sup>(5)</sup>	-0.36	0.24	2.00	0.73	0.14	0
HD 97320	-1.20	-0.85	-0.56 <sup>(6)</sup>	-0.66	0.21	2.32	0.43	0.17	0
HD 97916	-0.88	...	-0.06 <sup>(1)</sup>	-0.27	0.23	< 1.23	< -0.76	...	1
HD 103723	-0.82	-0.68	-0.33 <sup>(6)</sup>	-0.44	0.15	2.22	0.51	0.17	1
HD 106038	-1.30	...	-0.62 <sup>(3)</sup>	-0.70	0.21	2.55	1.37	0.12	1
HD 111980	-1.11	-0.76	-0.38 <sup>(6)</sup>	-0.50	0.29	2.31	0.67	0.13	1
HD 113679	-0.70	-0.43	-0.15 <sup>(6)</sup>	-0.28	0.32	2.05	0.87	0.12	1
HD 121004	-0.73	-0.42	-0.19 <sup>(2)</sup>	-0.27	0.28	< 1.18	0.94	0.15	1
HD 122196	-1.74	...	-1.07 <sup>(6)</sup>	-1.17	0.28	2.28	-0.51	0.14	0
HD 126681	-1.17	-0.72	-0.65 <sup>(4)</sup>	-0.70	0.30	1.48	0.90	0.12	0
HD 132475	-1.50	-1.09	-0.82 <sup>(4)</sup>	-0.91	0.27	2.23	0.62	0.13	1
HD 140283	-2.41	-1.61	-1.65 <sup>(3)</sup>	-1.73	...	2.16	-0.94	0.14	1
HD 160617	-1.78	-1.34	-1.24 <sup>(3)</sup>	-1.33	0.23	2.25	-0.41	0.12	1
HD 166913	-1.55	-1.16	-0.81 <sup>(4)</sup>	-0.90	0.30	2.32	0.27	0.14	0
HD 175179	-0.74	...	-0.13 <sup>(6)</sup>	-0.24	0.32	< 0.87	0.73	0.15	0
HD 188510	-1.67	...	-0.98 <sup>(5)</sup>	-1.02	0.31	1.48	-0.25	0.13	0
HD 189558	-1.15	-0.73	-0.54 <sup>(1)</sup>	-0.64	0.25	2.24	0.64	0.14	0
HD 195633	-0.64	-0.55	-0.16 <sup>(6)</sup>	-0.34	0.06	2.25	0.53	0.18	2
HD 205650	-1.13	-0.69	-0.48 <sup>(4)</sup>	-0.54	0.21	1.70	0.51	0.19	0
HD 298986	-1.33	-0.93	-0.70 <sup>(6)</sup>	-0.79	0.15	2.26	-0.04	0.12	1
CD -30°18140	-1.87	...	-1.09 <sup>(3)</sup>	-1.18	...	2.21	-0.35	0.15	1
CD -57°1633	-0.91	...	-0.51 <sup>(6)</sup>	-0.60	0.01	2.15	0.31	0.18	1
G 013-009	-2.28	...	-1.54 <sup>(3)</sup>	-1.65	...	2.21	-0.84	0.13	1
G 020-024	-1.92	...	-1.19 <sup>(3)</sup>	-1.30	...	2.19	-0.72	0.17	1
G 183-011	-2.08	...	-1.27 <sup>(6)</sup>	-1.36	...	2.21	-0.61	0.14	1

<sup>a</sup> Sources of equivalent width for O I triplet: (1) Cavallo et al. (1997), (2) Nissen & Schuster (1997), (3) Nissen et al. (2002), (4) Gratton et al. (2003), (5) Jonsell et al. (2005), (6) measured from archival UVES spectra (Programme ID 65.L-0507).

<sup>b</sup> Population membership: 0 – dissipative component; 1 – accretion component; 2 – thin disc.

**Table 4.** Comparison of Be abundances with those from literatures.

Star	(1)	(2)	(3)	(4)	(5)	This work
HD 76932	-11.04 ± 0.11	-11.45 ± 0.18	-11.21 ± 0.21	-11.17 ± 0.05	...	-11.27 ± 0.14
HD 132475	...	...	...	...	-11.43 ± 0.12	-11.38 ± 0.13
HD 140283	-12.78 ± 0.14	-13.07 ± 0.20	-12.91 ± 0.17	-13.08 ± 0.09	...	-12.94 ± 0.14
HD 160617	...	...	-12.90 ± 0.27	...	...	-12.41 ± 0.12
HD 166913	...	...	-11.77 ± 0.15	...	...	-11.73 ± 0.14
HD 189558	-10.99 ± 0.15	...	...	...	...	-11.36 ± 0.14
HD 195633	-11.21 ± 0.07	...	...	...	-11.34 ± 0.11	-11.47 ± 0.18

References: (1) Boesgaard & King (1993), (2) García López et al. (1995), (3) Molaro et al. (1997), (4) B99, (5) Boesgaard & Novicki (2006).

<sup>7</sup>Li abundances as a function of metallicity. We can see that six stars in our sample are obviously depleted in <sup>7</sup>Li and another two seem to be slightly depleted, while the star HD 106038 has an exceptionally high <sup>7</sup>Li abundance, about 0.3 dex higher than the Spite plateau (it also has an abnormally high Be abundance, see discussion in Sect. 5.2 for this star). Among those stars with depleted <sup>7</sup>Li, only one (HD 97916, denoted by filled inverse triangle in Fig. 7 and Fig. 8) is also depleted seriously in Be, while the rest (denoted by filled squares in Fig. 7 and Fig. 8) seem to have normal Be abundances at their metallicities.

Excluding HD 106038 and HD 97916 (abnormally high Be abundance and seriously depleted in Be, respectively; these two stars will not be included in the analysis of Be vs.

O trend either), the relation between Be and Fe abundances can be well represented by linear fitting

$$\log N(\text{Be}/\text{H}) = (1.15 \pm 0.07) [\text{Fe}/\text{H}] - (10.24 \pm 0.10)$$

One may note that HD 132475 and HD 126681 seem to deviate from the trend far beyond the uncertainties. If we exclude these two stars (see discussion in Sect. 5.2), the relationship will be

$$\log N(\text{Be}/\text{H}) = (1.10 \pm 0.07) [\text{Fe}/\text{H}] - (10.37 \pm 0.10)$$

Our result is in reasonable agreement with the result  $\log N(\text{Be}/\text{H}) = (0.96 \pm 0.04) [\text{Fe}/\text{H}] - (10.59 \pm 0.03)$  of B99, considering the relatively smaller metallicity range of our

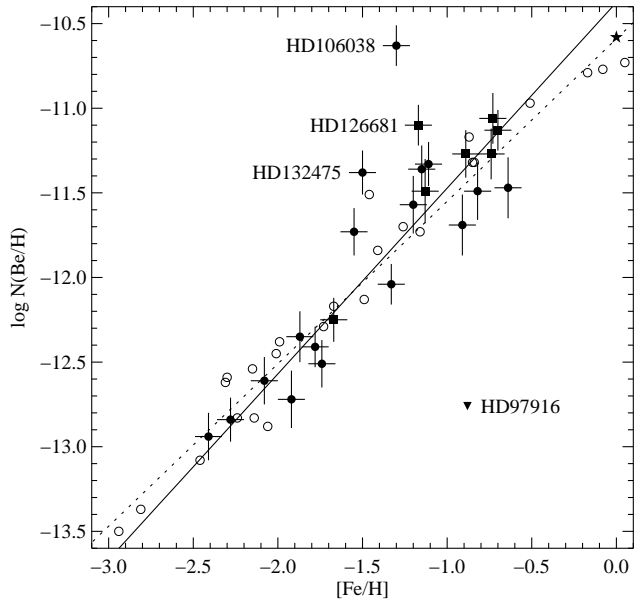


**Figure 7.** Be abundances against  $[\text{Fe}/\text{H}]$  (*filled circles*: stars without  ${}^7\text{Li}$  depletion; *filled squares*: stars with depleted  ${}^7\text{Li}$ ; *filled inverse triangle*: upper limit Be abundance for HD 97916; *filled star*: solar meteoritic Be abundance; *open circles*: data from B99). The solid line is the best linear fitting (not including HD 106038, HD 97916, HD 132475 and HD 126681) with a slope of 1.1 for our Be vs. Fe trend, while the dotted lines represents the best fitting for the B99 data.

sample. The overall increase of Be with Fe suggests that Be is enriched globally in the Galaxy.

As the yields of Be is believed to be correlated with CNO nuclei directly, it's more meaningful to investigate the relationship between Be and O abundances. Due to the inconsistent oxygen abundances based on the forbidden and triplet lines in our study, it is necessary to investigate their relations with Be abundance separately. Fig. 8 shows the trend of Be with O abundances. Again, the Be abundances increase linearly with increasing  $[\text{O}/\text{H}]$  both for the forbidden line (though with relatively large scatter partly due to the small sample number) and triplet lines. The relationships are best represented by

$$\begin{aligned} \log N(\text{Be}/\text{H}) &= (1.55 \pm 0.17) [\text{O}/\text{H}] - (10.29 \pm 0.15) & [\text{O I}] \\ \log N(\text{Be}/\text{H}) &= (1.36 \pm 0.09) [\text{O}/\text{H}] - (10.69 \pm 0.08) & \text{O I} \end{aligned}$$

If we exclude HD 132475 and HD 126681, the relationships will be

$$\begin{aligned} \log N(\text{Be}/\text{H}) &= (1.49 \pm 0.16) [\text{O}/\text{H}] - (10.42 \pm 0.15) & [\text{O I}] \\ \log N(\text{Be}/\text{H}) &= (1.30 \pm 0.08) [\text{O}/\text{H}] - (10.81 \pm 0.08) & \text{O I} \end{aligned}$$

Our result based on O I triplet lines is slightly flatter than the result  $\log N(\text{Be}/\text{H}) = (1.45 \pm 0.04) [\text{O}/\text{H}] - (10.69 \pm 0.04)$  of B99. This can be partly due to our smaller  $[\text{Fe}/\text{H}]$  range as mentioned above. Besides, the O abundances of B99 were averaged from the UV OH and infrared O I triplet lines. They thought that such a result (a slope of roughly 1.5 for Be vs. O) is neither consistent with the secondary process, nor the primary process. However, the secondary process added with some chemical evolution effects, such as an outflow of mass from the halo, indicates that there would

be a quadratic relation only at the very lowest metallicities and a progressive shallowing of the slope to disc metallicities, for example a slope of 1.5 between  $[\text{Fe}/\text{H}] = -2$  and  $-1$  (B99). So they suggested that this process is most consistent with their results.

As discussed above, [O I] forbidden line is the most reliable O abundance indicator for its insensitivity to the adopted stellar parameters as well as the non-LTE effects. Our oxygen abundances from [O I] 6300 Å line produces a ‘moderate’ slope 1.49 for the Be vs. O trend. However, Nissen et al. (2002) studied the effects of 3D model atmospheres on the derived O abundance from [O I] forbidden lines. They found that O abundances based on [O I] will decrease if 3D models are applied. Especially, the decreasing amplitude increases with decreasing metallicity (see fig. 6 and table 6 of Nissen et al. 2002). While 3D effects on Be II doublet are negligible according to Primas et al. (2000). This means that the slope will be closer to one than our present result when the 3D effects were considered for the [O I] forbidden lines. This implies that the Be production scenario is probably a primary process.

## 5.2 Special stars: hints on the Be production scenario

HD 106038 is very special for its exceptionally overabundance in Li and Be as mentioned before. Its Li abundance is 0.3 dex higher than the Li plateau, while its Be abundance is about 1.2 dex higher than that of normal stars with the same metallicity. The Be abundance of this star is even similar to the solar meteoritic value. Such a Be-rich star is extremely rare. Asplund et al. (2006) derived  $A(\text{Li}) = 2.49$  and Smiljanic et al. (2008) reported a Be abundance of  $\log N(\text{Be}/\text{H}) = -10.60$  for this star, both in good agreement with our results. In addition to Li and Be, Nissen & Schuster (1997) showed that this star also has obviously enhanced abundances of Si, Ni, Y, and Ba. Based on its special abundance pattern, Smiljanic et al. (2008) suggested that HD 106038 is most probably formed in the vicinity of a hypernova (HNe).

In addition to HD 106038, another two stars, namely HD 132475 and HD 126681, seem to stand out of the Be vs. Fe and Be vs. O trends distinctly. Their Be abundances are about 0.6 and 0.5 dex higher, respectively, than that of most stars with the same metallicities. Boesgaard & Novicki (2006) also found an abnormally high Be abundance for HD 132475 (0.5 dex above the normal stars at its metallicity). Their sample included another star BD+23°3912, which has very similar atmospheric parameters as HD 132475 but very different Be abundance. In fact, BD+23°3912 has a Be abundance matching perfectly the linear Be vs. Fe relation. Combined with another star HD 94028 also with excess Be abundance found by B99, Boesgaard & Novicki (2006) concluded that dispersion in Be abundances does exist at a given metallicity, which implies a local enrichment of Be in the Galaxy.

However, Pasquini et al. (2005) proposed that such dispersion could be mostly attributed to the scatter of Fe and O abundances, rather than Be, as we have mentioned in Sect. 1. Following Pasquini et al. (2005), we calculated the space velocities using the method presented by Johnson & Soderblom (1987), and determined the or-



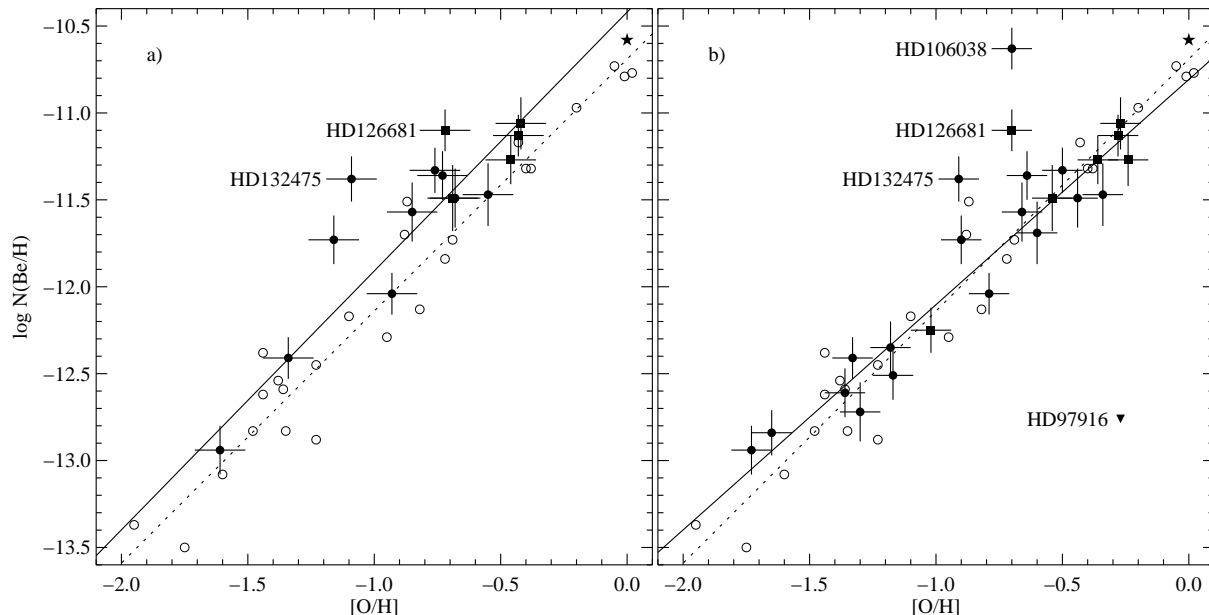


**Figure 8.** Be abundances as a function of  $[O/H]$ . a) Results from  $[OI]$  forbidden lines. b) Results from  $O\ I$  permitted lines. The symbols and lines have the same meaning as Fig. 7. Remember that  $O$  abundances of B99, for both of the two panels, are the mean abundances based on UV  $OH$  and infrared  $O\ I$  triplet lines.

bit parameters based on the Galactic mass model of Allen & Santillan (1991) for our sample stars. Input parameters, such as radial velocities, parallaxes and proper motions were obtained from the SIMBAD database. According to the criteria of Gratton et al. (2003), fifteen stars in our sample belong to the accretion component, nine stars belong to the dissipative component and one star belongs to the thin disc.

Fig. 9 shows  $[O/Fe]$  vs.  $[Fe/H]$  and  $[O/Fe]$  vs.  $\log N(Be/H)$  for our sample stars, based on the results from both  $[OI]$  forbidden line and  $O\ I$  triplet lines. One may find that no clear separation exists between the two components in the  $[O/Fe]$  vs.  $[Fe/H]$  diagram, though the accretion component shows a relatively larger scatter than the dissipative component. However, in the  $[O/Fe]$  vs.  $\log N(Be/H)$  diagram, the two populations are distinctly different, and especially, the accretion component shows a much larger scatter compared to the dissipative component. Our results agree well with the findings of Pasquini et al. (2005). They proposed that such results support the idea that the formation of the two components took place under significantly different conditions: an inhomogeneous, rapidly evolving ‘halo phase’ for the accretion component, and a more chemically homogeneous, slowly evolving ‘thick disc phase’ for the dissipative component. The large scatter of the accretion component in the  $[O/Fe]$  vs.  $\log N(Be/H)$  diagram may reflect the inhomogeneous enrichment in oxygen and iron of the halo gas. We note that, for our Be-rich stars, HD 106038 and HD 132475 belong to the accretion component, while HD 126681 belongs to the dissipative component. Another Be-rich star HD 94028, first discovered by B99 and later confirmed by Boesgaard & Novicki (2006), is also classified as a dissipative component star according to the definitions of Gratton et al. (2003). While the deviation of the accretion component stars could be due to the inhomogeneous enrichment in Fe and O of the halo gas, HD 126681 and HD 94028

cannot be interpreted in this way. However, one should keep in mind that stellar kinematics is only of statistical meaning in describing the Galactic populations. It has been shown by many previous work that substantial overlap exists between the halo and thick disc stars. Therefore, it is dangerous to attribute an individual star to one stellar population and accordingly derive a firm conclusion. Moreover, we didn’t find any distinct differences in the abundance pattern between HD 126681/HD 94028 and typical halo stars. So the possibility that dispersion in Be vs. Fe and Be vs. O trend originates from the inhomogeneous enrichment in Fe and O of the protogalactic gas cannot be excluded.

As an alternative, the scatter in Be can be interpreted by the so-called superbubble (SB) model (Higdon, Lingenfelter & Ramaty 1998; Parizot & Drury 1999; Parizot 2000b; Ramaty et al. 2000). The basic idea of the SB model is that repeated SNe occurring in an OB association can generate a superbubble, in which the CNO nuclei (ejected by SNe) mixed with some ambient, metal-poor material are accelerated onto the metal deficient material in the supershell and at the surface of the adjacent molecular cloud, and then broken into smaller atoms like Li, Be and B. The produced light elements are then mixed with other SNe ejecta as well as the ambient, metal-poor gas. However, such a mixing cannot be perfect, and new stars can form before all the massive stars explode or the induced light elements production occurs. As a result, scatter in the abundances of light elements for a given SB may occur (Parizot 2000a). Boesgaard & Novicki (2006) noted that Na, Mg, Si, Y, Zr, and Ba abundances of HD 132475 are typically 0.2 dex above the mean values of the other stars at that metallicity according to the results of Fulbright (2000, 2002). We also noted that Y and Ba abundances of HD 126681 are roughly 0.2 and 0.15 dex higher, respectively, than the mean values of the remaining sample as found by

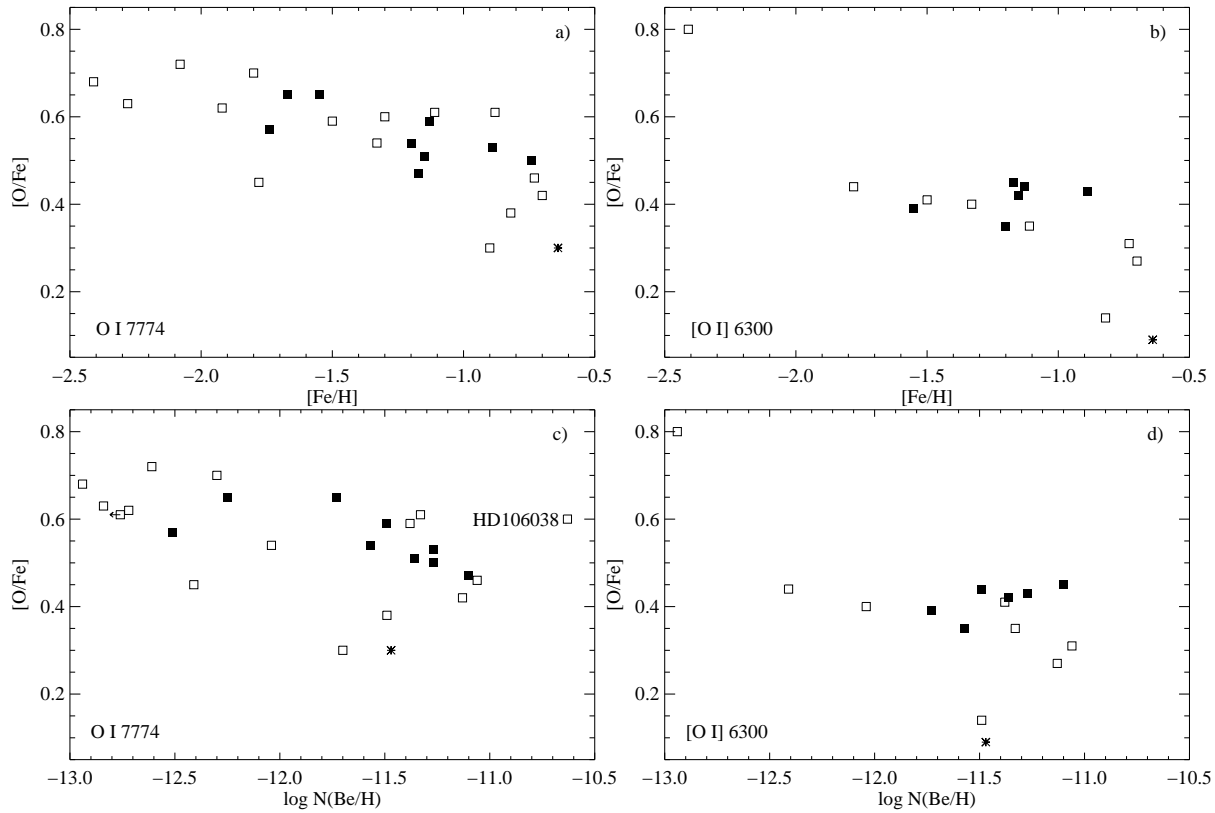


**Figure 9.** a)  $[O/Fe]$  vs.  $[Fe/H]$  based on O I triplet lines. b)  $[O/Fe]$  vs.  $[Fe/H]$  based on [O I] forbidden line. c)  $[O/Fe]$  vs.  $\log N(\text{Be}/\text{H})$  based on O I triplet lines. d)  $[O/Fe]$  vs.  $\log N(\text{Be}/\text{H})$  based on [O I] forbidden line. *Open squares* represent the accretion component, *filled squares* represent the dissipative component, and the *asterisk* represents the only thin disc star HD 195633 in our sample. The open square with a *left pointing arrow* represents the upper limit Be abundance for HD 97916.

Nissen & Schuster (1997), and the  $\alpha$ -elements of this star are in the upper range of their sample. Na and  $\alpha$ -elements are typical ejecta of SNeII, and Y, Zr, and Ba, though not very efficiently, can also be produced by the  $r$ -process in SNeII. It is probably that stars like HD 132475 and HD 126681 were formed from the material that underwent enrichment of light elements and SNeII ejecta but not plenty of dilution process in SBs. In addition, the SB model also predicts a primary process for the Be production, which is consistent with our Be vs. O trend.

Except for the possibilities stated above, some other scenarios for the overabundance of Be can be excluded. It is unlikely that the Be-rich stars were accreted from the satellite systems of our Galaxy. Shetrone, Cote & Sargent (2001) and Tolstoy et al. (2003) found that abundance patterns among the dwarf spheroidal (dSph) galaxies stars are remarkably uniform. We note that  $\alpha$ -elements and Y abundances of the dSph stars are obviously lower than the Be-rich stars. The possibility that the overabundance of Be in our Be-rich stars could be due to the accretion of a planet or planetesimals debris can also be excluded. If the excess Be in our Be-rich stars were accreted from some material having similar composition as chondrites meteorites, then the mass of the accreted iron would be even larger than the total mass of iron in the surface convective zone of the star, which is certainly impossible.

## 6 CONCLUSIONS

We have derived Be abundances for 25 main sequence and subgiant stars spanning the range  $-2.5 < [Fe/H] < -0.5$ . Relations between Be and Fe as well as Be and O are investigated. The Be vs. Fe trend can be well represented by a linear relation with a slope of 1.1. This result is in good agreement with that of B99, and suggests that Be is enriched globally in the Galaxy, as proposed by Suzuki & Yoshii (2001). Our Be abundances increase linearly with increasing  $[O/H]$  based on both the [O I] 6300 Å and O I triplet lines, but with slightly different slopes. O abundances based on O I triplet gives a slope of 1.30 between  $[Be/H]$  and  $[O/H]$ . This is a little flatter than the result of B99, which may be partly due to different metallicity range. The most reliable O abundance indicator, [O I] forbidden line gives a steeper relationship (a slope of 1.49). However, this slope will decrease if 3D effects are taken into account according to the results of Nissen et al. (2002), which means that the production process of Be is probably a primary process.

Moreover, we find some strong evidences for the intrinsic dispersion of Be abundances at a given metallicity. The special abundance pattern of HD 106038, especially its exceptionally high Be abundance, can be interpreted most consistently only if the material which formed HD 106038 was contaminated by the nucleosynthetic products of a HNe (Smiljanic et al. 2008). The deviations of HD 132475 and HD 126681 from the general Be vs. Fe and Be vs. O trend

can be interpreted by the SB model. However, the possibility that such dispersion originates from the inhomogeneous enrichment in Fe and O of the protogalactic gas cannot be excluded.

## ACKNOWLEDGMENTS

Thanks goes to the referee Luca Pasquini for constructive suggestions and comments. This work is supported by the National Natural Science Foundation of China under grants Nos. 10433010, 10521001 and 10778626. It has made use of the SIMBAD database, operated at CDS, Strasbourg, France.

## REFERENCES

- Allen C., Santillan A., 1991, *Rev. Mex. Astron. Astrofis.*, 22, 255
- Allende Prieto C., Lambert D. L., Asplund M., 2001, *ApJ*, 556, L63
- Alonso A., Arribas S., Martinez-Roger C., 1995, *A&A*, 297, 197
- Alonso A., Arribas S., Martinez-Roger C., 1996, *A&A*, 313, 873
- Anders E., Grevesse N., 1989, *Geochim. Cosmochim. Acta*, 53, 197
- Anstee S. D., O'Mara B. J., 1991, *MNRAS*, 253, 549
- Anstee S. D., O'Mara B. J., 1995, *MNRAS*, 276, 859
- Asplund M., García Pérez A. E., 2001, *A&A*, 372, 601
- Asplund M., Lambert D. L., Nissen P. E., Primas F., Smith V. V., 2006, *ApJ*, 644, 229
- Balachandran S. C., Bell R. A., 1998, *Nat*, 392, 791
- Barklem P. S., O'Mara B. J., Ross J. E., 1998, *MNRAS*, 296, 1057
- Bell R. A., Balachandran S. C., Bautista M., 2001, *ApJ*, 546, L65
- Boesgaard A. M., King J. R., 1993, *AJ*, 106, 2309
- Boesgaard A. M., Deliyannis C. P., King J. R., Ryan S. G., Vogt S. S., Beers, T. C., 1999, *AJ*, 117, 1549 (B99)
- Boesgaard A. M., Novicki M. C., 2006, *ApJ*, 641, 1122
- Cavallo R. M., Pilachowski C. A., Rebolo R., 1997, *PASP*, 109, 226
- Chmielewski Y., Brault J. W., Mueller E. A., 1975, *A&A*, 42, 37
- Dekker H., D'Odorico S., Kaufer A., Delabre B., Kotzlowski H., 2000, *SPIE*, 4008, 534
- Duncan D. K., Primas F., Rebull L. M., Boesgaard A. M., Deliyannis C. P., Hobbs L.M., King J. R., Ryan S. G., 1997, *ApJ*, 488, 338
- Fuhrmann K., Pfeiffer M., Frank C., Reetz J., Gehren T., 1997, *A&A*, 323, 909
- Fulbright J. P., 2000, *AJ*, 120, 1841
- Fulbright J. P., 2002, *AJ*, 123, 404
- García López R. J., Severino G., Gomez M. T., 1995, *A&A*, 297, 787
- García Pérez A. E., Asplund M., Primas F., Nissen P. E., Gustafsson B., 2006, *A&A*, 451, 621
- Gilmore G., Gustafsson B., Edvardsson B., Nissen P. E., 1992, *Nat*, 357, 379
- Gratton R. G., Carretta E., Claudi R., Lucatello S., Barbieri M., 2003, *A&A*, 404, 187
- Higdon J. C., Lingenfelter R. E., Ramaty R., 1998, *ApJ*, 509, L33
- Hinkle K. H., Lambert D. L., 1975, *MNRAS*, 170, 447
- Johnson D. R. H., Soderblom D. R., 1987, *AJ*, 93, 864
- Jonsell K., Edvardsson B., Gustafsson B., Magain P., Nissen P. E., Asplund M., 2005, *A&A*, 440, 321
- King J. R., Deliyannis C. P., Boesgaard A. M., 1997, *ApJ*, 478, 778
- Kiselman D., 2001, *New Astronomy Review*, 45, 559
- Kiselman D., Carlsson M., 1996, *A&A*, 311, 680
- Korn A. J., Shi J. R., Gehren T., 2003, *A&A*, 407, 691
- Kurucz R. L., 1992, *Rev. Mex. Astron. Astrofis.*, 23, 45
- Kurucz R. L., Furenlid I., Brault J., Testerman L., 1984, *Solar flux atlas from 296 to 1300 nm*, National Solar Observatory
- Magain P., 1989, *A&A*, 209, 211
- Molaro P., Bonifacio P., Castelli F., Pasquini L., 1997, *A&A*, 319, 593
- Nissen P. E., Schuster W. J., 1997, *A&A*, 326, 751
- Nissen P. E., Primas F., Asplund M., Lambert D. L., 2002, *A&A*, 390, 235
- Pasquini L., Bonifacio P., Randich S., Galli D., Gratton R. G., 2004, *A&A*, 426, 651
- Pasquini L., Galli D., Gratton R. G., Bonifacio P., Randich S., Valle G., 2005, *A&A*, 436, L57
- Pasquini L., Bonifacio P., Randich S., Galli D., Gratton R. G., Wolff B., 2007, *A&A*, 464, 601
- The Hipparcos and Tycho Catalogues, ESA SP-1200
- Parizot E., 2000, *A&A*, 356, L66
- Parizot E., 2000, *A&A*, 362, 786
- Parizot E., Drury L., 1999, *A&A*, 349, 673
- Primas F., Duncan D. K., Pinsonneault M. H., Deliyannis C. P., Thorburn J. A., 1997, *ApJ*, 480, 784
- Primas F., Asplund M., Nissen P. E., Hill V., 2000, *A&A*, 364, L42
- Ramaty R., Scully S. T., Lingenfelter R. E., Kozlovsky B., 2000, *ApJ*, 534, 747
- Rebolo R., Abia C., Beckman J. E., Molaro P., 1988, *A&A*, 193, 193
- Reeves H., Fowler W. A., Hoyle F., 1970, *Nat*, 226, 727
- Shetrone M. D., Cote, P., Sargent, W. L. W., 2001, *ApJ*, 548, 592
- Shi J. R., Gehren T., Zhang H. W., Zeng J. L., Zhao G., 2007, *A&A*, 465, 587
- Smiljanic R., Pasquini L., Primas F., Mazzali P. A., Galli D., Valle G., 2008, *MNRAS*, 385, L93
- Suzuki T. K., Yoshii Y., 2001, *ApJ*, 549, 303
- Takeda Y., 2003, *A&A*, 402, 343
- Thomas D., Schramm D. N., Olive K. A., Mathews G. J., Meyer B. S., Fields B. D., 1994, *ApJ*, 430, 291
- Tolstoy, E., Venn, K. A., Shetrone, M., Primas, F., Hill, V., Kaufer, A., Szeifert, T., 2003, *AJ*, 125, 707
- Valle G., Ferrini F., Galli D., Shore S. N., 2002, *ApJ*, 566, 252
- Wiese W. L., Fuhr J. R., Deters T. M., 1996, *J. Phys. Chem. Ref. Data*, Monograph No. 7
- Yi S. K., Kim Y. C., Demarque P., 2003, *ApJS*, 144, 259

This paper has been typeset from a  $\text{\TeX}$ / $\text{\LaTeX}$  file prepared by the author.